Some aspects of the theory of magnets with competing double exchange and superexchange interactions

D. I. Golosov*
The James Franck Institute, The University of Chicago, 5640 S. Ellis Avenue, Chicago, Illinois 60637
and Materials Science Division, Argonne National Laboratory, 9700 S. Cass Avenue, Argonne, Illinois 60439

M. R. Norman
Materials Science Division, Argonne National Laboratory, 9700 S. Cass Avenue, Argonne, Illinois 60439

K. Levin
The James Franck Institute, The University of Chicago, 5640 S. Ellis Avenue, Chicago, Illinois 60637
(Received 19 February 1998; revised manuscript received 26 June 1998)

In colossal magnetoresistance materials, ferromagnetic double exchange presumably coexists with a direct nearest-neighbor antiferromagnetic interaction. We construct a single-site mean-field theory that explicitly takes into account the different nature of carrier-mediated ferromagnetism vs Heisenberg-like superexchange. We find, in contrast to previous results in the literature, that the competition between these two exchange interactions leads to ferromagnetic or antiferromagnetic order with incomplete saturation of the magnetization (or sublattice magnetization), rather than spin canting. The associated experimental implications are discussed. [S0163-1829(98)08537-3]

I. INTRODUCTION

Recently, there has been a renewed interest (motivated by technological problems of microelectronics) in the properties of colossal magnetoresistance (CMR) manganese oxides.[1] The CMR behavior typically corresponds to an intermediate doping range, when these materials are ferromagnetic. The latter property is generally attributed to a conduction electron-mediated double exchange (DE) interaction.[2] In addition, there exists evidence[3–5] that suggests the presence of antiferromagnetic superexchange interactions of comparable scale. In this paper, we study the behavior of a classical magnet with competing double exchange and superexchange interactions, and show, in particular, that in an isotropic case the spin canting (which was previously suggested[6] to be a generic outcome of such a competition) can be stabilized only at very high fields and at very low temperatures.

Previous related calculations[6] have been performed for a strongly anisotropic model in which the inter- and intra-layer direct exchange constants have different signs.[7] Here, we assume that direct interactions have everywhere the same (antiferromagnetic) sign and magnitude. This is viewed as more appropriate for the $La_{1-x}Ca_xMnO_3$ perovskite family away from the $x=0$ endpoint, as well as for the layered manganates such as $La_{2-2x}Sr_{1+2x}Mn_2O_7$. In these compounds, pairs of stacked Mn-O planes form the bilayers, which are separated by poorly conducting layers of La(Sr)O (see Ref. 8). Since the lengths of the intralayer and interlayer bonds in a bilayer are roughly the same, the values of interlayer hopping coefficient and superexchange constant should be of the same order of magnitude as their intralayer counterparts. The observed interlayer canting[5] or canted correlations,[4] presumably caused by superexchange between the two layers of a bilayer complex, can be used to suggest relatively large values of superexchange within the layers as well. In view of the considerable interest in these layered systems, we consider primarily the two-dimensional (2D) lattice. By doing so, we expect to capture the basic magnetic properties of the layered compounds, while avoiding the cumbersome quantitative treatment of bilayers. We also note that our 2D results are qualitatively representative of the three-dimensional case as well.

We will see that the fact that the double exchange–superexchange competition occurs at *all* lattice bonds (i.e., in the 3D case, for in-, as well as out-of-plane interactions) leads to the enhancement of spin fluctuations. Lowest order (i.e., Hartree–Fock like) treatments are insufficient in this case. Therefore, in the present paper we introduce a new approach to the problem.

We construct a single-site mean field theory which explicitly takes into account the main feature of the present problem, namely, the carrier kinetic energy origin of the double exchange ferromagnetism. We note that the mean field schemes previously reported in the literature[6,9] essentially use an effective Heisenberg-like ferromagnetic exchange interaction to describe the double exchange. Such schemes would not adequately reflect the very different nature of the two competing interactions. It is of interest, then, to see how the results are changed if a more proper treatment of the double exchange is carried out. We begin with the standard Hamiltonian,[6,10] corresponding to an infinite on-site Hund's rule coupling:

$$\mathcal{H}=-\frac{t_0}{2}\sum_{\langle i,j\rangle}\cos\frac{\theta_{ij}}{2}\{c_i^\dagger c_j+c_j^\dagger c_i\}+\frac{J_{AF}}{S^2}\sum_{\langle i,j\rangle}\vec{S}_i\cdot\vec{S}_j-\frac{H}{S}\sum_i S_i^z. \tag{1}$$

Here, the first term is the kinetic energy of the carriers (which are represented by the fermion operators c_j where j is the site index). The second term corresponds to the nearest-neighbor antiferromagnetic ($J_{AF}>0$) exchange interaction between the classical ($S\gg 1$) core (localized) spins $\vec{S}_i$, and

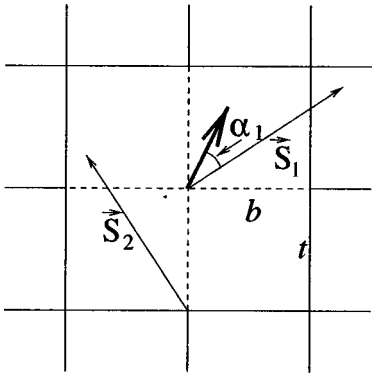

FIG. 1. Single-spin fluctuation in the ferromagnetic phase. The bold arrow represents the average magnetization, and the dashed lines correspond to the hopping amplitude b, which differs from the background hopping value t (solid lines).

the last term is the Zeeman energy of these spins in the external field H. The double exchange interaction results in the modulation of carrier hopping coefficients by the factors $\cos(\theta_{ij}/2)$, where $\cos\theta_{ij}=\vec{S}_i\cdot\vec{S}_j/S^2$. Since in the present work we restrict ourselves to a single-site mean-field treatment, we omit the additional phase factors that would result in Berry phase effects. We use units in which the bare hopping coefficient t_0, $\hbar$, k_B, μ_B, and the lattice spacing are all equal to unity.

Our mean-field framework is based on the exact solution of the single site problem, which is outlined in the following section. Details of the derivation are relegated to Appendix A, whereas the implications for the $T=0$ energetics are briefly discussed in Appendix B. Sec. III is concerned with the mean field treatment of different magnetic phases of the system, and the resultant mean field phase diagram is described in Sec. IV. We conclude with a brief discussion of the experimental relevance of our findings.[11]

II. EXACT SOLUTION OF THE SINGLE-SITE PROBLEM

The random distribution of localized spins leads in Eq. (1) to a highly disordered electronic hopping problem. Our mean-field treatment is based on evaluating the energy cost δF of a fluctuation of a single spin $\vec{S}_1$, embedded in an effective medium with a uniform average value of $\cos\theta_{ij}$. As we will see below [Eqs. (8), (13), and (19)], such a fluctuation gives rise to a difference between the values of hopping coefficient b from the site of the fluctuating spin $\vec{S}_1$ to the neighboring sites and the background hopping t ($t\neq b$); for clarity these parameters[12] are indicated schematically in Fig. 1.

The quantities b and t depend, in a self-consistent fashion, on the change δF_{DE} in the free energy, associated with the local change in hopping matrix elements $t\rightarrow b$. Such a local change, originating from a local spin fluctuation on the site $(0,0)$, gives rise to a perturbation,

$$V=-\frac{1}{2}(b-t)\{c^{\dagger}_{(0,0)}(c_{(0,1)}+c_{(1,0)}+c_{(0,-1)}+c_{(-1,0)})+\text{H. c.}\}, \tag{2}$$

in the carrier kinetic energy. This perturbation shifts the energy levels of individual carriers, thus resulting in a change in the total kinetic energy of the band. This kinetic energy contribution to δF, which can be evaluated following Refs. 13–15 (see Appendix A), is given by

$$\delta F_{DE}(b,t,T)=\int f(\epsilon)\xi(\epsilon)d\epsilon+\theta(b-t)[\varphi(z_0)-\varphi(-Dt)], \tag{3}$$

where the spectral shift function $\xi(\epsilon)$ takes values between -1 and 1, and is given by

$$\xi(\epsilon)=-\frac{1}{\pi}\text{Arg}\left\{b^2+(t^2-b^2)\epsilon\int\mathcal{P}\frac{\nu(\eta)d\eta}{\epsilon-\eta}+\pi\text{i}(t^2-b^2)\epsilon\nu(\epsilon)\right\}, \tag{4}$$

the bound state energy $z_0<-Dt$ is the root of

$$1+\frac{t^2-b^2}{t^2}\left\{-1+z\int\frac{\nu(\eta)d\eta}{z-\eta}\right\}=0, \tag{5}$$

$\nu(\epsilon)$ is the density of states,

$$\varphi(z)=-T\ln\left\{1+\exp\left(\frac{\mu-z}{T}\right)\right\},\quad f(z)=\frac{1}{\exp\left(\frac{z-\mu}{T}\right)+1}, \tag{6}$$

and μ is the chemical potential. Although we will apply Eqs. (3)–(5) only to the case of a 2D square lattice, they remain valid for a cubic lattice in 3D, as well as in the 1D case. The energy integrations are performed over the conduction band width, $-Dt<\epsilon,\eta<Dt$ where D is the dimensionality of the system. It should be stressed that it is because of the locality of the perturbation (2), which represents a lattice analogue of an s-wave scattering problem, that the quantity δF can be evaluated *exactly*.[13–16]

The second term in Eq. (3) is a contribution of a bound state that appears in the carrier spectrum for $b>t$ (when the perturbation may be viewed as a ''potential well''). In 2D, the binding energy of this state vanishes exponentially[17] as $b\rightarrow t$, whereas in 3D it has a threshold behavior. This bound state is related to one that causes the formation of magnetic polarons,[18] but it should be distinguished from the true magnetic polaron that is an extended object and cannot be treated within a single-site approach.

In order to gain additional intuition about the meaning of Eqs. (3)–(5), it is useful to calculate the energy cost of a single-spin fluctuation in various phases at $T=0$. This is discussed in Appendix B. This Appendix highlights the important differences between the double exchange and familiar Heisenberg direct exchange interactions.

For the purposes of the present work, the virtual crystal approximation, based on the parameters shown in Fig. 1, is expected to be appropriate as long as the carrier concentration is not too small. This is because the quantities of interest involve integration over carrier energies in the metallic phase. In order to extend this formulation beyond the single-site mean-field scheme, we note that multisite spin fluctua-

tions can also be treated as local perturbations following Ref. 14. This in principle allows one to study systematically the effects of correlations, by constructing an analogue of an impurity-concentration expansion. This procedure would also verify whether the virtual crystal approximation is a good starting point for studying other (e.g., transport) properties.

III. THE MEAN-FIELD-SCHEME

A. Ferromagnetic phase

In the ferromagnetic phase at $T>0$, the net energy cost of a single-spin fluctuation is (in $2D$) given by

$$\delta F_1 = \delta F_{DE}(b,t,T) + 4J_{AF}\langle\cos\theta_{12}\rangle_2 - H\cos\alpha_1 - 4J_{AF}\langle\cos\theta_{12}\rangle_{12} + H\langle\cos\alpha_1\rangle_1 . \quad (7)$$

Here, θ_{12} is the angle between the directions of the fluctuating spin $\vec{S_1}$ and any of the neighboring spins, denoted by $\vec{S_2}$ (we assume that spin fluctuations on different sites are statistically independent), and α_1 is the angle between $\vec{S_1}$ and the direction of magnetization, $\vec{M}$ (see Fig. 1). The angular brackets, $\langle\cdots\rangle_l$, are used to denote the average values over the Boltzmann probability distribution of spin $\vec{S_l}$, $w_l \propto \exp(-\delta F_l/T)$. We then find that $\langle\cos\theta_{12}\rangle_2 = M\cos\alpha_1$, and[19]

$$b^2 \equiv \langle\cos^2(\theta_{12}/2)\rangle_2 = (1+M\cos\alpha_1)/2,$$

$$t^2 \equiv \langle b^2\rangle_1 = (1+M^2)/2. \quad (8)$$

The magnetization has to be determined self-consistently as $M=\langle\cos\alpha_1\rangle_1$; generally, the latter equation has to be solved numerically.

In the ferromagnetic and antiferromagnetic phases, it is useful to construct a reference framework with which to compare our results. We define $J_{eff}(M)$ which represents an effective M- dependent exchange constant for a Heisenberg-like magnet. The appropriate exchange constant can be deduced by considering small spin fluctuations ($|\cos\alpha - M| \ll 1$), which correspond to small fluctuations in the hopping matrix elements ($|t-b| \ll t$). A perturbation expansion of Eq. (3) then leads to

$$\delta F_{DE}(b,t,T) \approx -2\frac{t-b}{t}\int \epsilon f(\epsilon)\nu(\epsilon)d\epsilon = 2(t-b)|E_0|, \quad (9)$$

at leading order[20] in T/t, where E_0 is the kinetic energy of the carriers for $t=1$. In the ferromagnetic state, using the corresponding formula for a Heisenberg ferromagnet [$\delta F = (4JM-H)(\cos\alpha_1 - M)$], we obtain

$$J_{eff}^{FM}(M) = J_{AF} - \frac{1}{8}|E_0|\sqrt{\frac{2}{1+M^2}}. \quad (10)$$

The second term in the above equation represents the DE contribution. This term, which is contained in other mean field schemes,[9,21] increases as M decreases. As a consequence, for moderately strong antiferromagnetic exchange interactions, when[22]

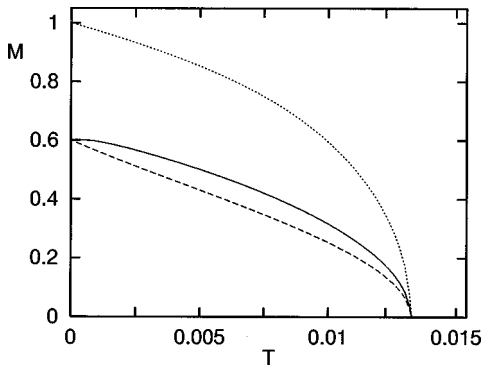

FIG. 2. Magnetization vs temperature in the ferromagnetic phase at $H=0$, $x=0.4$, and $J_{AF}=0.06$. The solid, dashed, and dotted lines correspond to the 2D DE– superexchange magnet, effective exchange approximation, and usual Heisenberg ferromagnet, respectively.

$$|E_0| < 8J_{AF} < \sqrt{2}|E_0|, \quad (11)$$

$J_{eff}^{FM}(M)$ changes sign as M varies from 0 to 1. This behavior has important consequences: it leads to a lack of saturation in the low temperature magnetization. Typical results for $M(T)$ are plotted in Fig. 2 for these moderately strong exchange interactions. Here the solid line represents the full mean-field calculation [which makes use of Eqs. (3) and (4)], while the dashed line corresponds to the effective exchange approximation. The dotted line represents the behavior of a conventional Heisenberg magnet with the same value of Curie temperature, and a constant nearest-neighbor exchange integral.

The lack of saturation seen in Fig. 2 can be understood as follows. In the paramagnetic phase, $M=0$ and, by virtue of Eqs. (10) and (11), the effective exchange constant has a negative (ferromagnetic) sign. As T decreases, the system undergoes a Curie transition at $T_C \approx 4|J_{eff}^{FM}(0)|/3$. Decreasing T further results in a decrease in the magnitude of spin fluctuations, i.e., in an increase of M. The latter is opposed by a *decrease* in $|J_{eff}^{FM}|$, leading to the softening of spin fluctuations. As a result, the effective exchange constant ''self-adjusts'' in such a way that it never becomes large in comparison with T, and even at low T the behavior of an effective exchange magnet is similar to that of a conventional Heisenberg magnet in a ''high-temperature'' regime of $T \sim T_C \sim J$. In this way, the nonvanishing thermal fluctuations do not allow the magnetization to reach its proper saturation value, $M_0=1$. At zero field, the value of magnetization as $T \to 0$ is instead given by[23]

$$M_0 = \sqrt{(E_0/J_{AF})^2/32 - 1} < 1. \quad (12)$$

These self-consistent changes in $|J_{eff}^{FM}|$ lead to inadequacies of the effective exchange approximation at low T. As may be seen in Fig. 2, the behavior obtained in this approximation differs significantly from that found using the full calculation of $M(T)$. This difference is due to the fact that when $J_{eff}^{FM} \lesssim T$ is small (in comparison with the electronic energy scales), quadratic terms [in $(t-b)/t$] dominate the physics. The details are discussed in Appendix C. Within the effective exchange approximation, strong fluctuations of *both* angular coordinates of each spin persist at low T. By contrast,

the full calculation shows that the fluctuations of the polar angle freeze out, $\cos\alpha_i \to M_0$. Independent fluctuations of the azimuthal angles of the spins, which persist down to $T \to 0$, appear to be an artifact of the single-site mean-field treatment. It is natural to expect that, at least in the classical case of $S \gg 1$, these azimuthal fluctuations also freeze out (albeit at a lower temperature than the polar ones) resulting in the formation of a multisublattice or spin-glass-like state with the net magnetization given approximately by Eq. (12).

B. Antiferromagnetic phase

The Néel antiferromagnetic state (of the metallic phase) can be treated similarly. We find $\langle\cos\theta_{12}\rangle_2 = -m\cos\alpha_1$, where α_1 is the angle formed by the spin $\vec{S}_1$ with its average direction and m is sublattice magnetization. Eqs. (8) are replaced by

$$b^2 = (1 - m\cos\alpha_1)/2, \quad t^2 = (1 - m^2)/2. \tag{13}$$

Instead of Eq. (10) we obtain

$$J_{eff}^{AFM}(m) = J_{AF} - \frac{1}{8}|E_0|\sqrt{\frac{2}{1-m^2}}. \tag{14}$$

It is easy to show that the Néel ordering arises for $J_{AF} > 2^{-5/2}|E_0|$ in zero field and at $T < T_N \approx 4J_{eff}^{AFM}(0)/3$. It always exhibits undersaturation of the sublattice magnetization: at $T \to 0$,

$$m \to m_0 = \sqrt{1 - (E_0/J_{AF})^2/32} < 1. \tag{15}$$

This undersaturation (which leads to a finite bandwidth) may be viewed as consistent with the presumed metallic state.

Numerical calculations yield the dependence of m on T, which is similar to $M(T)$ in the ferromagnetic phase and shows the same low-temperature features.

C. Canted phase

Our discussion thus far has not included the canted phase first proposed by De Gennes.[6] In our case, this is a two-sublattice (checkerboard) magnetic phase; the sublattice magnetizations have an equal magnitude m and form an angle 2γ with each other. In the present model, spin canting requires the presence of a magnetic field to break the high degeneracy that would otherwise occur. This degeneracy is related to the fact that at $H = 0$, the energy of the system depends solely on the values of the angles formed by the pairs of neighboring spins. All the neighbors of any spin $\vec{S}_1$ of sublattice I belong to sublattice II, and are parallel to each other at $T = 0$. Therefore, the energy of the system does not change as the spin $\vec{S}_1$ moves along any cone around their common direction. In the context of single site mean field approaches, the same holds at $T > 0$ for any cone around the *average* direction of the sublattice II spins. Thus, the probability distribution of the spin $\vec{S}_1$ will be axially symmetric with respect to the direction of the magnetization of sublattice II, with which the spin $\vec{S}_1$ will therefore be aligned on average (rather than with sublattice I). Thus, in the absence of perturbations (caused by next-nearest-neighbor exchange, anisotropy effects, quantum corrections, or small external fields) the canted state is destabilized, as a result of the underlying degeneracy.[24] Since it is site local,[25] its effects will persist as long as the energy scale of a perturbation *per individual spin* remains small in comparison with the characteristic energy, $k_B T$, of the thermal motion of a *single* spin.

To characterize the finite field canted state, we use the full non-perturbative expression (3). The mean-field framework of Eqs. (7) and (8) has to be modified to allow for a self-consistent determination of the *two* mean-field variables, m and γ. We now obtain two coupled mean field equations, which, as in the ferromagnetic phase, follow from the self-consistent definition of the sublattice magnetization m. For the component of $\langle\vec{S}_1\rangle$ parallel to the magnetization of sublattice I, we obtain

$$-\sin 2\gamma\langle\sin\alpha_1\cos\beta_1\rangle_1 + \cos 2\gamma\langle\cos\alpha_1\rangle_1 = m, \tag{16}$$

whereas the perpendicular component must vanish,

$$\cos 2\gamma\langle\sin\alpha_1\ \cos\beta_1\rangle_1 + \sin 2\gamma\langle\cos\alpha_1\rangle_1 = 0. \tag{17}$$

In writing Eqs. (16) and (17) we used a coordinate system with a polar axis parallel to the sublattice II magnetization. α_1 and β_1 are polar and azimuthal angles of the spin $\vec{S}_1$ in this frame, with $\beta_1 = 0$ corresponding to the spin $\vec{S}_1$ lying within the plane containing the two sublattice magnetizations.

For the net energy of a single-site fluctuation we now obtain, instead of Eq. (7),

$$\begin{aligned}\delta F_1 = {} & \delta F_{DE}(b,t,T) + 4J_{AF}m\cos\alpha_1 - 4J_{AF}m\langle\cos\alpha_1\rangle_1 \\ & - H(-\sin\gamma\ \sin\alpha_1\ \cos\beta_1 + \cos\gamma\cos\alpha_1) \\ & + H(-\sin\gamma\langle\sin\alpha_1\ \cos\beta_1\rangle_1 + \cos\gamma\langle\cos\alpha_1\rangle_1)\end{aligned} \tag{18}$$

whereas the values of the hopping coefficients [see Fig. 1 and Eq. (2)] are given by

$$b^2 = (1 + m\cos\alpha_1)/2, \quad t^2 = (1 + m^2\cos 2\gamma)/2. \tag{19}$$

The low-T canted state is found to be stable for $H > 0$ and $8J_{AF} > |E_0| + H$.

We begin with the case of relatively large bandfilling, corresponding to the undersaturated ferromagnetic behavior at $H = 0$ [see Eq. (11) and Fig. 2]. The solutions[26] of Eqs. (16) and (17) for typical parameters are illustrated in Fig. 3. One can see that, as $T \to 0$ in the canted phase, the sublattice magnetization m approaches its proper saturation value $m = 1$. Note that the ferromagnetic ($\gamma = 0$) solution to the mean-field equations is present at $H > 0$ as well. In Fig. 3, the corresponding magnetization, $M_{FM}(T)$, is represented by the dotted line. However, when the canted ($\gamma > 0$) solution exists, it corresponds to a lower value of the free energy. This is obvious from the fact that the net magnetization in the canted state $M_{CM}(T) \equiv -\partial F/\partial H = m\cos\gamma$ (dashed line in Fig. 3) is larger than $M_{FM}(T)$. The canted solution branches from the ferromagnetic one at temperature $T_1 \sim H$, when

$$4TM = H\langle\sin^2\alpha_1\rangle_1; \tag{20}$$

at this point the undersaturated ferromagnetic state undergoes a second-order spin-flip transition into the low-temperature canted state.[27] One can therefore conclude that

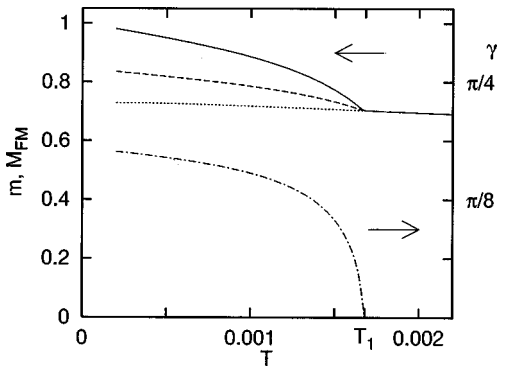

FIG. 3. The behavior of the sublattice (solid line) and net (dashed line) magnetizations in the canted state at $H=0.01$, $x=0.4$, and $J_{AF}=0.06$, in comparison with the magnetization of the ferromagnetic state (dotted line). The dashed-dotted line represents the results for the canting angle, γ.

undersaturation is representative of the generic low-temperature behavior of a double exchange-superexchange magnet.[28]

For smaller values of carrier concentration, at $H>0$ we find the spin-flop phase[29] of the undersaturated antiferromagnet, which evolves into the canted state via a smooth crossover at $T\sim H$, as shown in Fig. 4. The low-temperature region where the canting angle γ rapidly increases with T corresponds to the canted phase.

IV. MEAN-FIELD PHASE DIAGRAMS

Typical phase diagrams for the DE–superexchange magnet in (a,c) zero and (b,d) nonzero field are presented in Fig. 5. For t_0 of the order of an eV, our choice of parameters corresponds to reasonable values of $J_{AF}\lesssim 300$ K. In zero field (a,c), the solid line represents the phase boundary between paramagnetic (PM) and antiferromagnetic (AFM) or ferromagnetic (FM) metallic phases. For the values of parameters used in Fig. 5(a), the ordered phases are undersaturated at low T. For slightly smaller J_{AF} we find a critical value of bandfilling, x_1, which divides the saturated, $x>x_1$, and undersaturated regimes [see Fig. 5(c)]. At low temperatures and small concentrations, the undersaturated

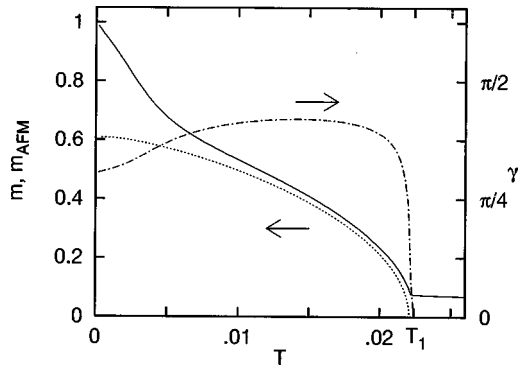

FIG. 4. Mean-field results for the case of strong superexchange, $J_{AF}=0.08$, $x=0.3$. The solid and dashed-dotted lines represent the result for the sublattice magnetization m and canting angle γ for $H=0.01$. The dotted line corresponds to the sublattice magnetization m_{AFM} of Néel AFM phase at $H=0$.

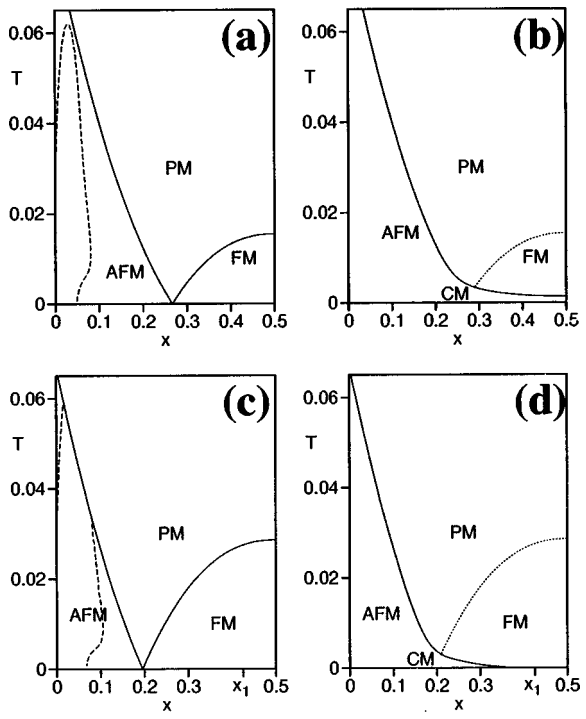

FIG. 5. Phase diagrams of the DE–superexchange magnet for $J_{AF}=0.06$ at $H=0$ (a) and $H=0.01$ (b), and for $J_{AF}=0.05$ at $H=0$ (c) and $H=0.01$ (d), showing the ferromagnetic, antiferromagnetic (flop phase at $H>0$), paramagnetic, and canted phases (FM, AFM, PM, and CM, respectively). The dashed line in (a) and (c) denotes the boundary of the thermodynamically unstable ($d\mu/dx<0$) region, and $x=x_1$ in (c) and (d) separates undersaturated ($x<x_1$) and saturated low-temperature regimes at $H=0$. The behavior of the system is symmetric with respect to quarter filling, $x=0.5$.

AFM state becomes thermodynamically unstable ($\partial\mu/\partial x<0$), signalling either the onset of a more complicated spin arrangement or phase separation (see Appendix C). The dashed line in Figs. 5(a) and 5(c) corresponds to the anticipated boundary of this region ($\partial\mu/\partial x=0$). We note that the possibility of phase separation in DE–superexchange systems has been suggested both by analytical studies[30] and numerical simulations.[31]

Figures 5(b) and 5(d) show that in the presence of a magnetic field the PM–FM transition is replaced by a smooth crossover (dotted line). The spin arrangement of the AFM phase becomes noncollinear (flop phase), and has the same symmetry properties as that of the canted phase, which becomes stable at lower T (replacing the $H=0$ undersaturated FM and AFM phases). The two are separated from the PM and FM region by a second-order phase transition at $T=T_1(x)$, which is represented by the solid line. At sufficiently small x the latter approaches the $H=0$ Néel transition line. The thermodynamic instability line [not shown in Figs. 5(b) and 5(d)] is only slightly affected by H.

V. DISCUSSION

We expect that our calculations are directly relevant to the quasi-2D layered materials $La_{2-2x}Sr_{1+2x}Mn_2O_7$. The existence of a strong superexchange interaction in this system is suggested by (i) relatively high values of Néel temperatures observed at the $x=1$ endpoint,[32] (ii) intra-layer antiferro-

magnetic correlations present near T_C (Ref. 3), (iii) interlayer (within the same bilayer) canting found at low temperatures[5] (see also Ref. 24) and interlayer canted correlations[4] present above T_C. The latter point is associated with the structure of the quasi-2D manganates, which was discussed in the Introduction.

The verification of the undersaturated behavior at low T remains an open question. It is not clear whether the materials $La_{2-2x}Sr_{1+2x}Mn_2O_7$, with $x=0.4$, lie within the region where the system exhibits undersaturated ferromagnetic behavior at low T, or outside of this region (in the latter case, we still expect thermal fluctuations to be stronger than in a Heisenberg magnet, due to the presense of superexchange). Some measurements of the absolute value of magnetization[33] in $x=0.4$ samples indicate undersaturation,[34,35] while others do not.[36]

We suggest that magnetic properties of the samples exhibiting undersaturation should be studied in the high-field, low-temperature regime of $T \lesssim H$. Our results [see Eq. (20)] indicate that the intralayer canted spin ordering should be stabilized in this region. Another important prediction of our theory is the unusual dependence of the effective ferromagnetic exchange constant on magnetization and hence on temperature [Eq. (10)]. While we did not study spin waves in the undersaturated low-temperature phase, it is clear that in such a situation the usual relationship between the low-T value of spin stiffness D_0 and the Curie temperature ($D_0 \propto T_C$) is no longer valid. This might help explain the recent experimental findings in perovskite manganates.[37] We propose that the magnetization dependence of the effective exchange constant (available through spin-wave measurements) should be studied in more detail in both 3D and 2D systems.

It should be noted that the presence of undersaturation in ferromagnetic and antiferromagnetic phases may well signal that in reality the system favours more complicated (e.g., spin-glass-like, cf. Ref. 36) spin ordering, that cannot be addressed within a single-site mean-field theory. The fact that there have been no observations of an *intralayer* spin canting in the layered compounds at $T \gg H$ is consistent with our results.

ACKNOWLEDGMENTS

This work has benefited from enlightening discussions that we had with many theorists and experimentalists, especially A. G. Abanov, A. Auerbach, A. V. Chubukov, M. I. Kaganov, M. Medarde, J. F. Mitchell, R. Osborn, R. M. Osgood, T. F. Rosenbaum, and A. E. Ruckenstein. We acknowledge the support of a Univ. of Chicago/Argonne National Lab. collaborative Grant, U. S. DOE, Basic Energy Sciences, Contract No. W-31-109-ENG-38, and the MRSEC program of the NSF under Grant No. DMR 9400379.

APPENDIX A: DERIVATION OF EQS. (3)–(5).

We begin by rewriting the local perturbation (2) as

$$V=-(b-t)(a_1^\dagger a_1 - a_2^\dagger a_2) \tag{A1}$$

in terms of the fermion operators,

$$a_{1,2}=\frac{1}{\sqrt{2}}c_{(0,0)} \pm \frac{1}{2\sqrt{2}}(c_{(1,0)}+c_{(0,1)}+c_{(-1,0)}+c_{(0,-1)}), \tag{A2}$$

which anticommute with each other. Perturbations of this form can be treated exactly by following I. M. Lifshits' theory of local perturbations.[13,14] Here we will use mainly the Green's functions (resolvent operators) approach of Refs. 14 and 16. We will, without loss of generality, consider the 2D case.

Perturbation (A1) results in a change of the net free energy of the carriers, which can be evaluated as

$$\begin{aligned}\delta F = \delta\Omega = -T\ \mathrm{Tr}\Bigg\{ &\ln\left[1+\exp\left(\frac{\mu-\mathcal{H}_{vc}-V}{T}\right)\right] \\ &-\ln\left[1+\exp\left(\frac{\mu-\mathcal{H}_{vc}}{T}\right)\right]\Bigg\} \\ &= \int_{-\infty}^{\infty}\varphi(\epsilon)[\tilde{\nu}_{tot}(\epsilon)-\nu_{tot}(\epsilon)]d\epsilon.\end{aligned} \tag{A3}$$

Here, $\varphi(\epsilon)$ is defined by Eq. (6), $\tilde{\nu}_{tot}(\epsilon)$ is the total (for the entire system) carrier density of states in the presence of perturbation (A1), and

$$\nu_{tot}(\epsilon)=N\nu(\epsilon)=\frac{4N}{\pi^2}\frac{1}{2t+|\epsilon|}\mathcal{K}\left(\frac{2t-|\epsilon|}{2t+|\epsilon|}\right), \tag{A4}$$

[where $\mathcal{K}(x)$ is the complete elliptic integral and N is the number of lattice sites] is the total density of states corresponding to the unperturbed virtual-crystal band Hamiltonian

$$\mathcal{H}_{vc}=-\frac{t}{2}\sum_{\langle i,j\rangle}(c_i^\dagger c_j + c_j^\dagger c_i), \tag{A5}$$

with the spectrum, $\epsilon(\vec{q})=-t(\cos q_x+\cos q_y)$. The perturbed density of states $\tilde{\nu}_{tot}(\epsilon)$ may include δ-function peaks corresponding to the discrete levels which split off downwards from the bottom of the band. As we shall see below, only one discrete level may appear in the present problem,[38] and after integration by parts the free-energy change (A3) can be rewritten[13,16] in the form of Eq. (3) (where the first term on the r.h.s. accounts for the contribution of the continuous part of the spectrum). We note that Eq. (3) is an example of a Krein trace formula. The quantity

$$\xi(\epsilon)=-\int_{-\infty}^{\epsilon}(\tilde{\nu}_{tot}(\eta)-\nu_{tot}(\eta))d\eta \tag{A6}$$

is called the *spectral shift function* because of its relationship to the perturbation-induced shifts of the energy levels in the case of a discrete (or discretized) unperturbed spectrum.[13] It can be evaluated as

$$\xi(\epsilon)=\frac{1}{\pi}\mathrm{Im}\ \mathrm{Tr}\{\ln G(\epsilon-i0)-\ln G_0(\epsilon-i0)\}, \tag{A7}$$

where the operators $G_0(\epsilon)=(\epsilon\cdot\hat{1}-\mathcal{H}_{vc})^{-1}$ and

$$G(\epsilon)=(G_0^{-1}(\epsilon)-V)^{-1}=(\hat{1}-G_0(\epsilon)V)^{-1}G_0(\epsilon) \tag{A8}$$

are the Green's functions for the unperturbed and perturbed Hamiltonians, respectively, and $\hat{1}$ is the identity operator. Equation (A7) yields $d\xi/d\epsilon = -\,\mathrm{Im\,Tr}\{G(\epsilon - i0) - G_0(\epsilon - i0)\}/\pi$. In turn,

$$\begin{aligned}\mathrm{Tr}(G-G_0) &= \mathrm{Tr}\{(\hat{1}-G_0V)^{-1}G_0VG_0\}\\ &= \mathrm{Tr}\{(\hat{1}-G_0V)^{-1}G_0^2V\}\\ &= \frac{d}{d\epsilon}\,\mathrm{Tr\ ln}(\hat{1}-G_0V)\\ &= \frac{d}{d\epsilon}\,\mathrm{ln\ Det}(\hat{1}-G_0V),\end{aligned} \tag{A9}$$

where we used the fact that the operators $(\hat{1}-G_0V)^{-1}$ and G_0V commute with each other. Therefore,[14,16]

$$\xi(\epsilon) = -\frac{1}{\pi}\,\mathrm{Arg\ Det}\{\hat{1}-G_0(\epsilon - i0)V\}. \tag{A10}$$

Since, according to Eq. (A1), the perturbation V is nothing but the sum of two projection operators, it is convenient to evaluate the r.h.s. of Eq. (A10) in a basis which includes the states $|1\rangle$, $|2\rangle$, annihilated by the operators $a_{1,2}$ [see Eq. (A2)]. In this basis, the determinant reduces to that of a 2×2 matrix, and one obtains

$$\begin{aligned}\xi = -\frac{1}{\pi}\,\mathrm{Arg}\{&1+(b-t)(I_{11}-I_{22})-(b-t)^2[\mathrm{Det}(I_{ij})\\ &-\pi^2\,\mathrm{Det}(C_{ij})]+\pi i[(b-t)(C_{11}-C_{22})+(b-t)^2\\ &\times(C_{12}I_{21}+C_{21}I_{12}-C_{11}I_{22}-C_{22}I_{11})]\}.\end{aligned} \tag{A11}$$

Here the quantities I_{ij} and C_{ij}/π with $i,j=1,2$ denote, respectively, the real and imaginary parts of the matrix elements $\langle i|G_0(\epsilon - i0)|j\rangle$. Explicitly, we find

$$C_{11}(\epsilon) = \frac{1}{2}\,\nu(\epsilon)\left(1-\frac{\epsilon}{t}\right)^2,$$

$$C_{12}(\epsilon) = C_{21}(\epsilon) = \frac{1}{2}\,\nu(\epsilon)\left(1-\frac{\epsilon^2}{t^2}\right),$$

$$C_{22}(\epsilon) = \frac{1}{2}\,\nu(\epsilon)\left(1+\frac{\epsilon}{t}\right)^2, \quad I_{ij}(\epsilon) = \int_{-2t}^{2t}\mathcal{P}\frac{C_{ij}(\eta)\,d\eta}{\epsilon-\eta}.$$

We then obtain[39]

$$\mathrm{Det}(C_{ij}) = 0,\ \ \mathrm{Det}(I_{ij}) = -\frac{1}{t^2}+\frac{\epsilon}{t^2}\int_{-2t}^{2t}\mathcal{P}\frac{\nu(\eta)\,d\eta}{\epsilon-\eta}, \tag{A12}$$

etc., and finally, Eq. (A11) takes form of Eq. (4). The latter can be conveniently rewritten as

$$\pi\,\cot\{\pi\xi(\epsilon)\} = -\frac{1}{\epsilon\nu(\epsilon)}\,\frac{b^2}{t^2-b^2}-\frac{1}{\nu(\epsilon)}\int\mathcal{P}\frac{\nu(\eta)\,d\eta}{\epsilon-\eta}, \tag{A13}$$

where the branch of arc cot should be selected in a way which respects both the continuity of $\xi(\epsilon)$ (Ref. 16) and the fact that $\xi(\epsilon)\equiv 0$ for $b=t$.

We note that the r.h.s. of the Eq. (A13) has the form $F(\epsilon)/\nu(\epsilon)$, diverging as $\nu(\epsilon)\to 0$. Therefore its possible values below the bottom of the band are $\mp\infty$, corresponding either to $\xi(\epsilon)=-1$ or to $\xi(\epsilon)=0$. The case of $\xi(\epsilon)=-1$ corresponds to the values of ϵ between the bottom of the band and the bound state when the latter is present, while for ϵ smaller than all the eigenvalues of $\mathcal{H}$ (continuous and discrete alike) the spectral shift function vanishes, $\xi(\epsilon)=0$. The change between these two values, which corresponds to the bound state, can occur only at $\epsilon = z_0$, where z_0 satisfies the equation $F(z)=0$. The latter condition yields Eq. (5). Although it appears rather intuitive, this consideration of the bound-state problem can be substantiated by a direct calculation along the lines of Ref. 15.

Interestingly, in Ref. 13 the notion of a finite trace of certain operators in an infinte-dimensional Hilbert space [see Eq. (A3)] was essentially introduced for the first time. Mathematical studies of related issues were initiated by M. G. Krein,[16] and since then the Krein trace formulas remain an active research topic of functional analysis.

APPENDIX B: SATURATED PHASES AT $T=0$

In this Appendix, we present some numerical and analytical results related to the phases which saturate at low T (i.e., the phases with values of magnetization or sublattice magnetization approaching unity at $T\to 0$). This being the simplest application of Eqs. (3)–(5), it provides insight into the meaning of these equations which are crucial for the present paper. The undersaturated phases at low T will be considered in the Appendix C.

We will assume that in the ground state, all the pairs of neighboring spins form the same angle 2γ and that each spin forms an angle γ with the z axis (thus, $\gamma=0$ corresponds to the ferromagnetic phase, and $\gamma>0$ – to the two-sublattice canted state of De Gennes). Then the energy of the system at $T=0$ can be written as[6]

$$F^{(0)}/N = -|E_0|\cos\gamma + 2J_{AF}\cos 2\gamma - H\cos\gamma, \tag{B1}$$

Here, E_0 is the energy of electrons for $t=1$. Let us now consider a single-spin perturbation of the ground state corresponding to the change of the polar angle value of a spin $\vec{S_1}$ from γ to α. The energy difference between this configuration and the ground state is given by

$$\begin{aligned}\delta F^{(0)}(\alpha) = \delta F_{DE}[b(\alpha),t,0] &+ 4J_{AF}[\cos(\alpha+\gamma)-\cos 2\gamma]\\ &- H(\cos\alpha-\cos\gamma),\end{aligned} \tag{B2}$$

where $\delta F_{DE}[b(\alpha),t,0]$ is given by Eqs. (3)–(5) with $t=\cos\gamma$ and $b=\cos\{(\alpha+\gamma)/2\}$. By minimizing $E^{(0)}$ with respect to $\cos\gamma$, we find[6] that the saturated ferromagnetic phase is stable at $|E_0|+H\geqslant 8J_{AF}$. In this case one can use Eq. (9) to obtain the value of $\delta F^{(0)}$ for $\alpha\ll 1$:

$$\delta F^{(0)}(\alpha) = -(4J_{eff}^{(0)}-H)(1-\cos\alpha), \tag{B3}$$

where the effective exchange constant (cf. Sec. III) is given by $J_{eff}^{(0)} = J_{AF} - |E_0|/8$. In the case of pure double exchange,

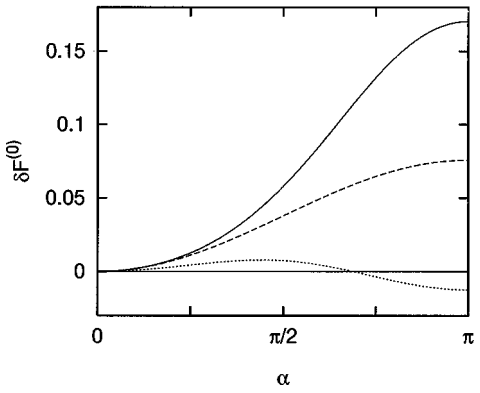

FIG. 6. Single-spin perturbation energy $\delta F^{(0)}(\alpha)$ in the ferromagnetic state at $T=0$ in zero field, for $x=0.4$ and $J_{AF}=0.04$. Solid line represents the exact result [see Eq. (B2)], while the dashed line corresponds to the effective exchange approximation, Eq. (B3). The dotted line represents the exact result for $\delta F^{(0)}(\alpha)$ at $x=0.15$, $J_{AF}=0.025$.

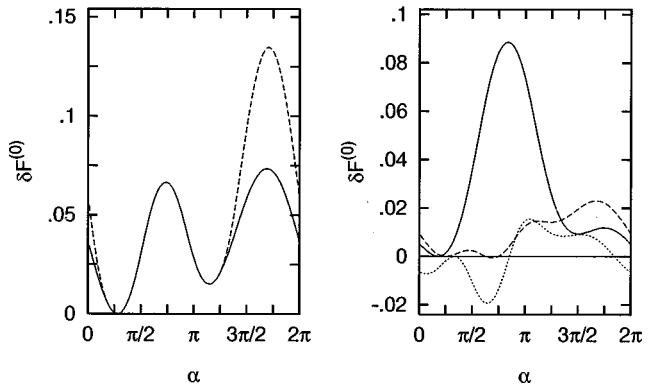

FIG. 7. The function $\delta F^{(0)}(\alpha)$ in the canted state at $T=0$. The left panel corresponds to $x=0.4$, $J_{AF}=0.08$, $H=0.01$. The dashed line represents the band contribution. In the right panel, $\delta F^{(0)}(\alpha)$ is plotted for $J_{AF}=0.06$ and $H=0.01$ at $x=0.4$ (solid line), $x=0.25$ (dashed line) and $x=0.15$ (dotted line).

$J_{AF}=0$, and for sufficiently large carrier concentration $x \gtrsim 0.1$, the effective exchange approximation is in fact adequate even for large values of α. Numerically, the difference between Eqs. (B2) and (B3) at $\alpha=\pi$ does not exceed 15–20%. This relative difference (which reflects the different physics of the double exchange and Heisenberg exchange) becomes more pronounced at large $J_{AF} \sim |E_0|/8$ (see Fig. 6). At smaller concentrations, $x<0.27$ in 2D, and at sufficiently large values of J_{AF}, we find $\delta F^{(0)}(\pi)<0$ (dotted line in Fig. 6). This means that the energy of the system can be lowered by flipping a single spin, and the ferromagnetic state becomes metastable.

For larger values of J_{AF}, corresponding to $J_{AF}>(|E_0|+H)/8$, the canted state with

$$\cos\gamma = \frac{|E_0|+H}{8J_{AF}} \tag{B4}$$

emerges at $T=0$, $H>0$ (see Sec. III regarding the latter condition). In this case, the energy of small single-spin perturbations is quadratic in $|b-t|/t \ll 1$,

$$\delta F^{(0)}(\alpha) \approx \left\{ \left(|E_0| + \frac{16HJ_{AF}^2}{64J_{AF}^2 - (|E_0|+H)^2} \right) \times \cos\gamma - \int_{-2}^{\mu} \left(\int_{-2}^{2} \mathcal{P} \frac{\nu(\eta)\, d\eta}{\eta - \epsilon} \right) \epsilon^2 \nu(\epsilon)\, d\epsilon \right\} \times (\alpha-\gamma)^2 \tan^2\gamma. \tag{B5}$$

Note that the effective exchange approximation, which is based on the first order [in $(b-t)/t$] perturbation theory result (9), is inapplicable. The typical results for $\delta F^{(0)}(\alpha)$ in the canted state are shown in Fig. 7 (left panel), where the dashed line represents the contribution of the band (first) term on the r.h.s. of Eq. (3); one can see that the bound state noticeably lowers energies of fluctuations with $\alpha \approx 2\pi - \gamma$.

The origins of instabilities of the canted state which appear in our single-site treatment are illustrated in the right panel of Fig. 7, where functions $\delta F^{(0)}(\alpha)$ at different band fillings x for $J_{AF}=0.06$, $H=0.01$ are plotted. We see that as one lowers the bandfilling from $x=0.4$ to $x=0.25$, $\delta F^{(0)}(\pi-\gamma)$ becomes negative, so that the total energy can be lowered by flipping a single spin of sublattice I to the direction antiparallel to that of sublattice II spins, and the canted state is metastable. As one further lowers concentration to $x=0.15$, the sign of $\partial^2 \delta F^{(0)}(\alpha)/\partial\alpha^2$ at $\alpha=\gamma$ changes, signalling the instability of the canted phase. Indeed, since in 2D the principal-value integral on the r.h.s. of Eq. (B5) diverges at $\epsilon \to -2$, the prefactor in front of $(\alpha-\gamma)^2$ in Eq. (B5) is negative at small x. At $H \to 0$, this coefficient changes sign at $x \approx 0.215$ [cf. Appendix C, and Eq.(C4)].

APPENDIX C: THE UNDERSATURATED FERROMAGNETIC STATE AT LOW *T*

In this Appendix, we present results on the breakdown of the effective exchange approximation and on the low-temperature stability of the undersaturated ferromagnet.

At $H=0$, the first term in the expansion of δF_1 [see Eq. (7)] in powers of $\delta M = \cos\alpha_1 - M$,

$$\delta F_1(M,T) = A(M,T)\,\delta M + B(M,T)(\delta M)^2 + \ldots, \tag{C1}$$

is proportional to the effective exchange constant, $A = 4J_{eff}^{FM}(M)$. If the temperature is not too low, this linear term (which generates the effective exchange approximation) provides a qualitatively reasonable approximation for δF_1 (see Fig. 2). Thus, the system behaves as a Heisenberg ferromagnet with an M-dependent exchange constant. As explained in Sec. III, for sufficiently large values of J_{AF} [see Eq. (11)], J_{eff}^{FM} decreases with decreasing T so that $|J_{eff}^{FM}(M(T))| \lesssim T$. Within the effective exchange approximation, $M_0 - M(T) \propto T$ at $T \to 0$.

The effective exchange approximation, however, breaks down at low T, when the second term on the r.h.s. of Eq. (C1) becomes dominant. This situation (which is depicted in Fig. 8) is due to the fact that the coefficient B,

$$B(M,T) \approx \frac{M^2}{4t^3} \left\{ |E_0| - \int_{-2}^{\mu_0} \epsilon^2 J_0(\epsilon)\, \nu_0(\epsilon)\, d\epsilon \right\} \tag{C2}$$

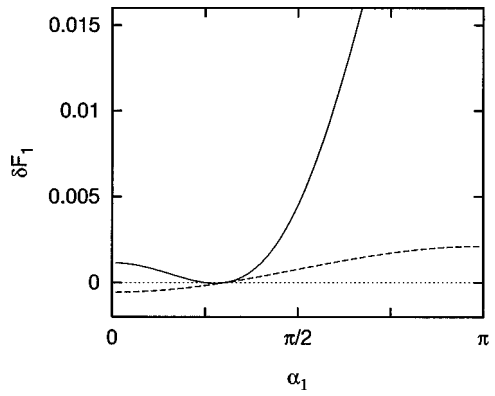

FIG. 8. The energy cost δF_1 of a single-site fluctuation in the ferromagnetic case at low-T (see Appendix C). The pronounced minimum of $\delta\Omega$ at the average value of the polar angle α represents a sharp difference from the effective exchange approximation (dashed line) and causes the fluctuations of α (but not of the azimuthal angle, β) to freeze out at low T. The plot corresponds to $H=0$, $x=0.4$, $T=0.002$, and $J_{AF}=0.06$.

does not vanish at $M\to M_0$. In Eq. (C2), t is given by Eq. (8), and

$$J_0(\epsilon)=\int_{-2}^{2}\mathcal{P}\frac{\nu_0(\epsilon)}{\eta-\epsilon}d\eta, \tag{C3}$$

μ_0 and $\nu_0(\epsilon)$ are the chemical potential and the density of states in the unrenormalized ($t=1$) band.

At $M_0-M(T)\ll\sqrt{T}$, the linear in δM term in Eq. (C1) can be omitted altogether. We then find that $\delta M=0$ corresponds to an energy minimum if

$$|E_0|>\int_{-2}^{\mu_0}\epsilon^2 J_0(\epsilon)\nu_0(\epsilon)d\epsilon. \tag{C4}$$

In this case, the fluctuations of $\cos\alpha$ at low T are confined to the vicinity of M_0 (see Fig. 8).

When the inequality (C4) is not satisfied, the undersaturated FM phase is expected to become unstable at low T. It is easy to see that in any dimensionality $D>1$, the inequality (C4) is violated at $x\to 0$. This follows from the fact that, when ϵ approaches the bottom of the band,

$$-\epsilon J_0(\epsilon)=1-\int_{-D}^{D}\mathcal{P}\frac{\eta\nu_0(\eta)}{\eta-\epsilon}d\eta>1. \tag{C5}$$

On the other hand, in 2D or in higher dimensions, the inequality (C4) is always satisfied for sufficiently large x. It is easy to see that the ratio of the l.h.s. of Eq. (C4) to the r.h.s. increases as the maximum of $\nu_0(\epsilon)$ at $\epsilon=0$ becomes more pronounced. Let us consider the extreme case of a constant density of states, $\nu_0(\epsilon)\equiv 1/4$, and calculate both sides of Eq. (C4) at $x=0.5$. We find:

$$|E_0|=\frac{1}{2},\quad \int_{-2}^{0}\epsilon^2 J_0(\epsilon)\nu_0(\epsilon)d\epsilon=\frac{1}{2}\left(\frac{2}{3}\ln 2+\frac{1}{3}\right),$$

so that the condition (C4) indeed is valid. Numerical calculations show that in 2D, inequality (C4) holds for $x>x_c\approx 0.215$. We anticipate that the value of x_c in 3D is lower. We also expect that, similarly to the ferromagnetic or canted state at $T=0$ (see Appendix B), the undersaturated FM state at low T may become metastable at values of x slightly above x_c.

We note that the similar stability conditions for the antiferromagnetic and canted (at small H) phases also take the form of Eq. (C4). These should be distinguished from the weaker thermodynamic stability condition $d\mu/dx>0$ mentioned in Sec. IV. The latter condition (in the antiferromagnetic, canted, and undersaturated ferromagnetic phases at $H,T\to 0$) can be rewritten as

$$\frac{d}{dx}(\mu_0 t)=\frac{1}{8J_{AF}}\frac{d}{dx}(\mu_0|E_0|)=\frac{1}{8J_{AF}}\left\{\frac{|E_0|}{\nu_0(\mu_0)}-\mu_0^2\right\}>0, \tag{C6}$$

and in 2D holds at $x>0.165$. In writing Eq. (C6), we assumed that $M\to M_0$ at $T\to 0$; note that this may be incorrect whenever the inequality (C4) is violated.

*Electronic address: golosov@franck.uchicago.edu

[1] For a review, see A. P. Ramirez, J. Phys. Condens. Matter **9**, 8171 (1997).

[2] C. Zener, Phys. Rev. **82**, 403 (1951).

[3] T. G. Perring, G. Aeppli, Y. Moritomo, and Y. Tokura, Phys. Rev. Lett. **78**, 3197 (1997).

[4] S. Rosenkranz, R. Osborn, J. F. Mitchell, L. Vasiliu-Doloc, J. W. Lynn, S. K. Sinha, and D. N. Argyriou, J. Appl. Phys. **83**, 7348 (1998); R. Osborn, S. Rosenkranz, D. N. Argyriou, L. Vasiliu-Doloc, J. W. Lynn, S. K. Sinha, K. E. Gray, and S. D. Bader (unpublished).

[5] K. Hirota, Y. Endoh, Y. Moritomo, Y. Maruyama, and A. Nakamura (unpublished).

[6] P.-G. De Gennes, Phys. Rev. **118**, 141 (1960).

[7] In this model (which was chosen to fit the known magnetic behavior of the undoped perovskite La Mn O_3), ferromagnetic intralayer exchange results in ferromagnetic ordering within the lattice layers.

[8] Y. Moritomo, A. Asamitsu, H. Kuwahara, and Y. Tokura, Nature (London) **380**, 141 (1996); T. Kimura, Y. Tomioka, H. Kuwahara, A. Asamitsu, M. Tamura, and Y. Tokura, Science **274**, 1698 (1996), and references therein.

[9] A. J. Millis, P. B. Littlewood, and B. I. Shraiman, Phys. Rev. Lett. **74**, 5144 (1995); N. Furukawa, J. Phys. Soc. Jpn. **63**, 3214 (1994).

[10] P. W. Anderson and H. Hasegawa, Phys. Rev. **100**, 675 (1955).

[11] The preliminary results were reported by the present authors in J. Appl. Phys. **83**, 7360 (1998).

[12] Our choice of virtual crystal parametrization does not include but could be generalized to incorporate a $(\pi,0,0)$-type AF ordering.

[13] I. M. Lifshits, Usp. Mat. Nauk **7**, No. 1, 171 (1952), and references therein; a brief account of this work is given by I. V. Krasovskii and V. I. Peresada, Fiz. Nizk. Temp. **23**, 79 (1997) [Low Temp. Phys. **23**, 59 (1997)].

[14] I. M. Lifshits, S. A. Gredeskul, and L. A. Pastur, *Introduction to the Theory of Disordered Systems* (Wiley, New York, 1988), Chap. 5.

[15] I. M. Lifshits, Zh. Eksp. Teor. Fiz. **17**, 1076 (1947).

[16] M. G. Krein, *Topics in Differential Equations and Operator Theory* (Birkhäuser, Basel, 1983), pp. 107–172, and references therein.

[17] For $(b-t)/t \ll 1$, we find $z_0+2t \approx -4t\exp\{-\pi t/[2(b-t)]\}$.

[18] E. L. Nagaev, Zh. Éksp. Teor. Fiz. Pis'ma Red. **6**, 484 (1967) [JETP Lett. **6**, 18 (1967)]; Zh. Éksp. Teor. Fiz. **54**, 228 (1968) [Sov. Phys. JETP **27**, 122 (1968)].

[19] We characterize the background by the average hopping *probability*, $\langle |t_{ij}|^2 \rangle$. This appears to be a more natural choice, in comparison with the average hopping amplitude, $\langle |t_{ij}| \rangle$, of Ref. 6.

[20] The small $[\sim T/(\mu+2t)]$ thermal correction to the total band energy, originating from the smearing of the Fermi distribution function, is omitted for simplicity in the text of the present paper. It was, however, taken into account in our numerical calculations (see Figs. 2–5).

[21] S. K. Sarker, J. Phys. Condens. Matter **8**, L515 (1996).

[22] Eq. (11) refers to the $H=0$ case. At $H>0$, either ferromagnetic or paramagnetic (with $M \sim H$) solution to the mean-field equations formally exists at all values of E_0. As M increases from $0+$ to 1, the quantity $J_{eff}^{FM}(M)-H/(4M)$ changes sign if $8J_{AF} > |E_0| + 2H$; the latter condition replaces Eq. (11).

[23] In the presence of a magnetic field, M_0 is given by the root of equation $4MJ_{eff}^{FM}(M)=H$. Thus, the noticeable increase in M_0 requires very high fields, $H \sim J_{AF} \sim t_0 x$.

[24] This argument can be generalized for a DE–superexchange bilayer, where the four-sublattice canted structure is degenerate with respect to simultaneous motion of the *pairs* of spins. This should generally lead to an undersaturated ferromagnetic ordering within each layer, with some interlayer canting (cf. Ref. 5).

[25] Another example of a classical spin system with site-local continuous degeneracy is provided by the Kagomé antiferromagnet [see: J. T. Chalker, P. C. W. Holdsworth, and E. F. Shender, Phys. Rev. Lett. **68**, 855 (1992); A. V. Chubukov, Phys. Rev. Lett. **69**, 832 (1992)].

[26] In evaluating the average values in Eqs. (16) and (17), the integrations over the azimuthal angle β_1 can be performed analytically.

[27] If the transition temperature T_1 is sufficiently low, so that $M_0 - M(T_1) \ll T_1$, the associated susceptibility jump is given by $\chi_{canted} - \chi_{ferro} \approx 1/[4T_1(1-M_0^2)]$.

[28] While it is not clear whether undersaturation is present in the case of quantum spins, we note that this would be not inconsistent with the results obtained for the somewhat similar case of quantum ferrimagnets [see: A. V. Chubukov, K. I. Ivanova, P. Ch. Ivanov, and E. R. Korutcheva, J. Phys. Condens. Matter **3**, 2665 (1991)].

[29] The spin-flip transition between the flop phase and a paramagnet occurs at temperature T_1, which is again given by Eq. (20), $T_1 \to T_N$ at $H \to 0$ (note that in an antiferromagnet, $M \propto H$ in weak fields).

[30] E. L. Nagaev, Usp. Fiz. Nauk **166**, 833 (1996) [Phys. Usp. **39**, 781 (1996)], and references therein.

[31] S. Yunoki, J. Hu, A. L. Malvezzi, A. Moreo, N. Furukawa, and E. Dagotto, Phys. Rev. Lett. **80**, 845 (1998); S. Yunoki and A. Moreo, Phys. Rev. B **58**, 6403 (1998).

[32] M. Medarde and J. F. Mitchell (private communication).

[33] One should distinguish between Rietveld measurements (Ref. 34) and SQUID magnetometer results (Refs. 35 and 36), which can be affected by possible interlayer canting.

[34] J. F. Mitchell, D. N. Argyriou, J. D. Jorgensen, D. G. Hinks, C. D. Potter, and S. D. Bader, Phys. Rev. B **55**, 63 (1997).

[35] R. Seshadri, M. Hervieu, C. Martin, A. Maignan, B. Domenges, B. Raveau, and A. N. Fitch, Chem. Mater. **9**, 1778 (1997).

[36] Y. Moritomo, Y. Maruyama, T. Akimoto, and A. Nakamura, Phys. Rev. B **56**, R7057 (1997).

[37] J. A. Fernandez-Baca, P. Dai, H. Y. Hwang, C. Kloc, and S.-W. Cheong, Phys. Rev. Lett. **80**, 4012 (1998).

[38] Since we are interested in the low-temperature case of $T \ll \epsilon_F$, we do not take into account the other discrete level arising near the *top* of the conduction band.

[39] We make use of the facts that $\nu(\epsilon)=\nu(-\epsilon)$ and $\int_{-2t}^{2t} \nu(\epsilon) d\epsilon = 1$.